

## Non-Invasive Bio-Impedance Imaging and Sensing for Medical Diagnostics and Industrial Applications

To cite this article: Ramesh Kumar *et al* 2024 *J. Electrochem. Soc.* **171** 107510

View the [article online](#) for updates and enhancements.

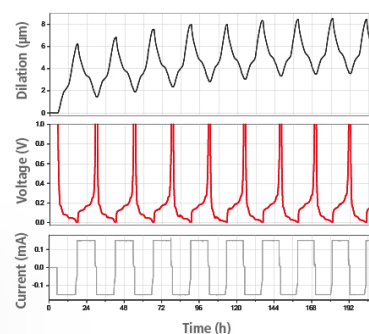
### You may also like

- [Evaluation of adjacent and opposite current injection patterns for a wearable chest electrical impedance tomography system](#)  
Lin Yang, Zhijun Gao, Chunchen Wang et al.
- [Wearable pulmonary monitoring system with integrated functional lung imaging and chest sound recording: a clinical investigation in healthy subjects](#)  
I Frerichs, R Paradiso, V Kilintzis et al.
- [13th International Conference on Electrical Bioimpedance and 8th Conference on Electrical Impedance Tomography \(Graz, Austria, 29 August–2 September 2007\)](#)  
Richard H Bayford and Hermann Scharfetter

## Watch Your Electrodes Breathe!

Measure the Electrode Expansion in the Nanometer Range with the ECD-4-nano.

- ✓ Battery Test Cell for Dilatometric Analysis (Expansion of Electrodes)
- ✓ Capacitive Displacement Sensor (Range 250  $\mu\text{m}$ , Resolution  $\leq 5$  nm)
- ✓ Detect Thickness Changes of the Individual Half Cell or the Full Cell
- ✓ Additional Gas Pressure (0 to 3 bar) and Temperature Sensor (-20 to 80° C)



**EL-CELL**<sup>®</sup>  
electrochemical test equipment

See Sample Test Results:



Scan me!

Download the Data Sheet (PDF):



Scan me!

Or contact us directly:

+49 40 79012-734

sales@el-cell.com

www.el-cell.com



# Non-Invasive Bio-Impedance Imaging and Sensing for Medical Diagnostics and Industrial Applications

Ramesh Kumar,<sup>1,2</sup> Ratneshwar Kumar Ratnesh,<sup>3,z</sup> Rajeev Kumar Chauhan,<sup>4</sup>  
Ashok Kumar,<sup>5</sup> Manish Kumar Singla,<sup>1,6</sup> and Ramji Gupta<sup>7</sup>

<sup>1</sup>Department of Interdisciplinary Courses in Engineering, Chitkara University Institute of Engineering & Technology, Chitkara University, Punjab140401, India

<sup>2</sup>Jadara University Research Center, Jadara University, Jordan

<sup>3</sup>Department of Electronics & Communication Engineering, Meerut Institute of Engineering & Technology, Meerut, UP, 250005, India

<sup>4</sup>Department of Electronics & Communication Engineering, IIMT College of Engineering, Greater Noida, UP, 201310, India

<sup>5</sup>Department of Electronics and communication Engineering, National Institute of technology, Hamirpur HP, 177005, India

<sup>6</sup>Applied Science Research Center, Applied Science Private University, Amman, 11931, Jordan

<sup>7</sup>Department of Electronics and Communication Engineering, Parul Institute of Engineering and Technology, Faculty of Engineering and Technology, Parul University, Vadodra, Gujarat, 391760, India

Bio-impedance-based imaging technique stands at the intersection of medical/industrial imaging techniques and is also known as electrical impedance tomography (EIT), imparting a non-invasive, value-powerful approach for imaging biological tissues and procedures. We begin by elucidating the essential standards underlying EIT, focusing on the size of impedance variations inside an object (plastic pipe) to reconstruct its inner conductivity distribution. Subsequently, we delve into the numerous programs of EIT across numerous fields and discuss recent experimental strategies and advancements aimed at mitigating these boundaries, such as novel electrode configurations, advanced reconstruction algorithms, and incorporation of complementary imaging modalities. Finally, we underscore the importance of experimental research in advancing the capabilities and packages of EIT as a valuable device in industrial monitoring, specifically in bedside tracking, process pipelines, tank monitoring and also used for other medical or industrial detection, even as additionally exploring its rising roles in commercial and environmental applications.

© 2024 The Electrochemical Society ("ECS"). Published on behalf of ECS by IOP Publishing Limited. All rights, including for text and data mining, AI training, and similar technologies, are reserved. [DOI: [10.1149/1945-7111/ad830b](https://doi.org/10.1149/1945-7111/ad830b)]

Manuscript submitted August 8, 2024; revised manuscript received September 3, 2024. Published October 15, 2024.

The idea of examining any object's internal properties through the use of current, voltage distribution, and resistivity measurements is not new, but a particular method is known as Electrical Impedance Tomography (EIT), which is based on the above parameters like current distribution, resistivity, and voltages.<sup>1</sup> EIT is an evolving medical imaging technique that provides a unique view of the object's internal properties. Unlike traditional imaging methods such as X-rays or MRIs, EIT is completely non-invasive and radiation-free. It works by measuring electrical inertia, a property that determines how easily electricity flows through tissues.<sup>2</sup> By applying electricity to the body surface and introducing small electric fields, EIT can reconstruct an image of the internal impedance distribution.<sup>2,3</sup> In 1978, it was separately proposed for geophysical applications (Lytle & Dines) and medical imaging (Henderson & Webster) (Daily & Ramirez, 2000).<sup>1</sup> Since then, advancements in computing power have enabled large-scale 3D EIT analysis, further accelerated by improved methods for solving the inverse problem.<sup>4,5</sup>

EIT offers a new way to visualize the interior of an object without disrupting its normal function. It's particularly useful for aqueous-based processes like liquid mixing, solid-liquid interactions, and cyclonic separation.<sup>6</sup> EIT provides a non-invasive, cost-effective, and non-destructive method for visualization and measurement.<sup>7-10</sup> The images generated by this technique can enhance process understanding, enabling real-time control to optimize energy consumption and maximize product yield.<sup>2,3</sup> This holds particular promise for medical research, as the electrical properties of air and water are quite different. Research indicates that EIT can provide real-time information about internal changes, which can help optimize and identification of internal structures, which is based on impedance.<sup>11,12</sup> Integrating EIT with other imaging modalities such as Magnetic Resonance Imaging (MRI) or Computed Tomography (CT) holds significant potential for enhancing diagnostic accuracy and providing a more comprehensive view of internal structures. By combining EIT's ability to measure electrical impedance variations with the detailed anatomical insights provided

by MRI or the high-resolution cross-sectional images from CT, clinicians and engineers can achieve a more holistic understanding of complex conditions and materials.<sup>6,7</sup> This multimodal approach leverages the strengths of each technique EIT's sensitivity to changes in electrical properties, MRI's superior soft tissue contrast, and CT's detailed structural imaging to deliver richer, more precise diagnostic information. For instance, in medical diagnostics, this integration can improve the detection and characterization of tumors by correlating electrical impedance changes with detailed anatomical and functional data.<sup>11,12</sup> Similarly, in industrial applications, it can enhance the monitoring of dynamic processes and the assessment of structural integrity by combining real-time electrical measurements with high-resolution structural imaging. The fusion of these modalities offers a powerful tool for advancing both medical diagnostics and industrial process management, providing a deeper and more accurate analysis of internal conditions.

EIT has increasingly become a valuable tool in diverse industrial applications because of its non-invasive nature and capacity to provide real-time, spatially-resolved statistics. In process monitoring, it enables continuous observation of material flow, mixing processes, and reaction dynamics in real-time. This capability allows for immediate detection of deviations from optimal process conditions, and optimization of industrial processes.<sup>7</sup> For instance, in chemical reactors, EIT can visualize the distribution of reactants and products, providing insights that help optimize reaction conditions and improve yield. The Pipeline analysis is another significant industrial application of EIT. By continuously monitoring of the pipelines, EIT helps in detecting blockages, leaks, or changes in the flow profile in pipelines.<sup>6</sup> EIT contributes to enhanced safety and efficiency in these industrial settings by providing critical, real-time information that aids in the early detection of issues, process optimization, and proactive maintenance. Its ability to deliver detailed internal insights without disrupting operations makes it an invaluable tool for modern industrial applications.<sup>6,7</sup>

In this paper, EIT works by reconstructing the resistance distribution within a pipe or vessel, creating an image that reflects the distribution of different materials present. This image reconstruction relies on specific algorithms, which significantly impact its

quality and accuracy. However, a major challenge arises from the inherent nature of EIT image reconstruction: it's an ill-posed and non-linear inverse problem. This means that small variations in the measured voltages can lead to significant distortions in the reconstructed image, making it difficult to accurately represent the true distribution of materials within the pipe. Additionally, existing algorithms often suffer from limitations like lengthy computation times and severe image distortion. Therefore, developing faster and more precise reconstruction algorithms is crucial for EIT to achieve its full potential.

### Literature Review

The chosen research area has been actively investigated for several years. To gain a thorough understanding, various techniques were used as reference points. Specifically, Guizhi et al. (2007) presented a new EIT system with 128 electrodes. This system allows for impedance change detection and 3D imaging, ultimately determining the electrical conductivity and permittivity distribution within an object based on surface measurements.<sup>12</sup> Their implementation of the back-projection algorithm successfully reconstructed conductivity distribution images. Furthermore, Fang-Ming Yu et al. (2007) explored the concept of "pseudo electrode driven patterns" for EIT.<sup>13</sup> By strategically changing the measurement points of the physical electrodes, they were able to create expanded "pseudo electrodes." This approach utilizes  $N$  electrodes to obtain  $N(N-1)/2$  individual measurements. This method expands the measurement sites, potentially increasing spatial resolution and reducing the required number of physical electrodes, ultimately simplifying the EIT system design.<sup>14</sup>

Several studies have explored the application of neural networks in EIT image reconstruction: based on conductivity images reconstructed using AC-EIT and compared them to traditional IC-EIT data with their proposed eight-coil configuration. This system offers stable conditions for future comparisons of different imaging modes and coil configurations.<sup>12</sup> Adler (1996) proposed a novel method for reconstructing changes in internal conductivity distribution and electrode movement between measurements. They used a finite element model for both the forward and inverse calculations, successfully reconstructing images from simulated 2D and 3D scenarios with conductivity variations and electrode movements.<sup>15-17</sup> Denisov et al. (2005) investigated the use of neural networks, specifically Hopfield networks and perceptron, for solving linear and non-linear problems in various tomography applications. While perceptron offer advantages like high data processing rates, Hopfield networks are typically used for linear problems. This work highlights the potential benefits of optical methods for implementing neural networks in tomography, but acknowledges the complexity of the implementation architecture.<sup>18</sup>

Several studies have explored novel image reconstruction algorithms for EIT: Hun (2016) proposed a new algorithm based on Radial Basis Function (RBF) neural networks. This method utilizes simulated EIT data to reconstruct images, but like other techniques, faces the inherent challenges of EIT image reconstruction: the ill-posed and non-linear nature of the inverse problem, leading to difficulties in accurately representing the true material distribution. Additionally, existing algorithms often suffer from long computation times and significant image distortion.<sup>19</sup> Argyrou et al. (2010) investigated a new image reconstruction technique using Artificial Neural Networks (ANNs) intended for use with a rotating phantom system for SPECT imaging. While their ANN-based approach yielded promising results for a  $27 \times 27$  matrix, it may not be suitable for higher dimensions or complex patterns due to limitations in the network's capabilities.<sup>20,21</sup> Shaomin Zhou and Jouko Halttunen (2003) developed a low-cost system for measuring pulp consistency profiles using EIT. Their system employs a modified Newton-Raphson algorithm for image reconstruction, offering a non-invasive and cost-effective alternative to conventional methods. However, further research is needed to reduce data collection time and simplify

the iterative algorithm for online monitoring applications.<sup>22</sup> Jennifer Mueller et al. (2002) presented a non-iterative reconstruction algorithm for 2D EIT based on Nachman's mathematical proof. While this method offers a direct approach, it is limited to specific conductivity conditions with two derivatives and requires smoothing on virtual organ boundaries. Additionally, it is not applicable for 3D reconstructions.<sup>23</sup>

Recent advances in EIT highlight important innovations in both platforms and techniques. Xia et al. (2024) investigate a combination of Neural Architecture Search (NAS) and deep image prior techniques, presenting a new approach to image reconstruction in EIT applications and demonstrating how NAS can better simulate deep learning to provide impedance imaging with accuracy and efficiency and offers promising directions for future research in this field (Xia et al., 2024).<sup>24</sup> Meanwhile, Nur Rifai et al. (2024) contribute to developing FPGA-based EIT systems with their results using a planar sensor system characterized by a dual response Howland constant-current pump and programmable measurements. This work highlights the system's versatility and accuracy and marks an important step forward in practical EIT applications.<sup>25</sup> Author Pietrzyk et al. (2024) highlight the potential of EIT to address challenging medical imaging challenges, demonstrating its effectiveness and adaptability in the clinical setting (Pietrzyk et al., 2024).<sup>26</sup> Collectively, these studies highlight the continued development of EIT technology, pushing both the theoretical and practical aspects of this imaging approach.

### Methodology for EIT

EIT is a non-invasive imaging technique that reconstructs internal conductivity distributions by measuring impedance variations. The core principle of EIT involves the relationship between electrical impedance, which includes resistance and reactance, and the physical properties of the object under study. Specifically, EIT focuses on the resistive component of impedance, which is inversely related to electrical conductivity. By measuring how impedance varies across different electrode configurations, EIT infers changes in conductivity within the object, allowing for the reconstruction of internal structures.<sup>1-3</sup>

The process of EIT involves solving two main problems: the forward and inverse problems. The forward problem predicts the electrical potential distribution on the surface of an object based on a known conductivity distribution, using partial differential equations (PDEs) and numerical methods like finite element modelling.<sup>1,2</sup> The inverse problem, which is inherently ill-posed, reconstructs the internal conductivity from measured boundary impedances using optimization techniques. To address this ill-posedness, regularization methods such as Tikhonov and Total Variation Regularization are employed. Effective data acquisition, including electrode placement and current injection patterns, is crucial for accurate imaging. Overall, EIT's ability to reconstruct conductivity distributions hinges on solving these problems and applying appropriate regularization and measurement strategies.

EIT operates by passing a constant current through a material and measuring the resulting voltage distribution on its surface, such as shown in Fig. 1. This voltage distribution reflects the internal resistivity (resistance to current flow) within the material. However, it's important to understand that multiple internal resistivity configurations can produce the same surface voltage pattern.<sup>27,28</sup> To overcome this ambiguity and accurately determine the internal resistivity distribution, the EIT system stimulates the material in various ways. Figure 1 depicts a simple EIT setup with 16 electrodes surrounding a circular object.<sup>29</sup> Here, a current ( $I$ ) is injected through a pair of opposing electrodes, while the voltage ( $V_i$ ) is measured between each neighboring pair of electrodes around the perimeter. Once all voltage measurements are complete, the current injection points are shifted to the next neighboring pair, maintaining their opposing configuration. This process repeats until a total of 208 voltage measurements are collected.<sup>29,30</sup>

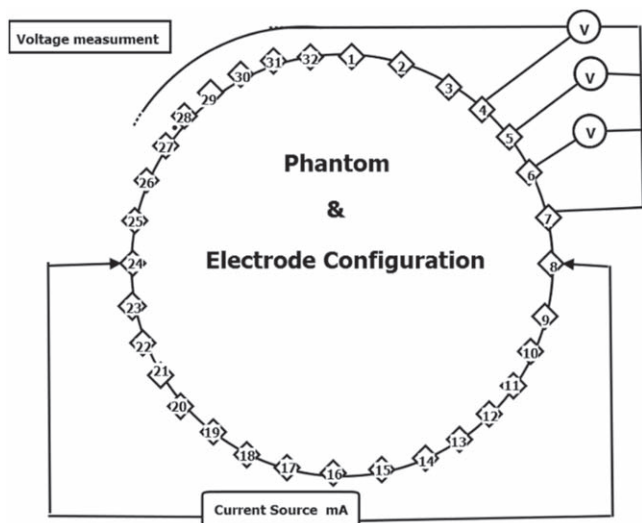


Figure 1. EIT Diagram with phantom and electrode configuration.

EIT is a novel imaging technique that allows visualizing the interior of an object without disrupting its normal operation. This makes it particularly useful for studying aqueous-based processes like liquid mixing, solid-liquid interactions, and cyclonic separation. EIT offers several advantages: it's non-invasive, cost-effective, non-destructive, and non-radiating, providing a visualization and measurement tool simultaneously.<sup>31</sup> The images generated by EIT can enhance process understanding, enabling real-time control to optimize energy consumption and maximize product yield.<sup>2,3</sup> This technology has garnered significant research interest globally and has witnessed rapid development.

The core principle of EIT involves reconstructing the resistance distribution within an object, creating an image that reflects the

distribution of different materials present. This image reconstruction relies on specific algorithms, which significantly impact its quality and accuracy. However, a major challenge arises from the inherent nature of EIT: it's an ill-posed and non-linear inverse problem.<sup>31,32</sup> This means that small variations in the measured voltages can lead to significant distortions in the reconstructed image, making it difficult to accurately represent the true distribution of materials within the object. Additionally, existing algorithms often suffer from limitations like lengthy computation times and severe image distortion.<sup>33</sup> Therefore, developing faster and more precise reconstruction algorithms is crucial for EIT to achieve its full potential.

**Data acquisition methods.**—Initially, it is an example of a bio-impedance-based monitoring technique, which is related to EIT. In EIT, many methods are used for data acquisition for any phantom or object, such as shown in Figs. 2(A)–2(D). That object may be industrial as well as medical and agriculture-based applications

**Neighbouring method.**—This method utilizes adjacent electrodes for current injection and voltage measurements in a cylindrical volume conductor equipped with 16 equally spaced electrodes (as depicted in the Fig. 2b). The current is initially applied between electrodes 1 and 2, resulting in the highest current density between them and rapidly decreasing with distance. Subsequently, the voltage is measured sequentially between all other adjacent electrode pairs (3–4, 4–5, etc.). The first four such measurements are shown in Fig. 2b, with all 13 measurements being independent (indicated by the shaded area for the voltage measurement between electrodes 6 and 7). The next set of 13 voltage measurements is obtained by injecting current through electrodes 2 and 3, as shown in Fig. 2b. This process repeats, ultimately acquiring a total of 208 voltage measurements for a 16-electrode system. However, due to the principle of reciprocity, where interchanging current and voltage electrodes yields identical results, only 104 measurements are truly independent.

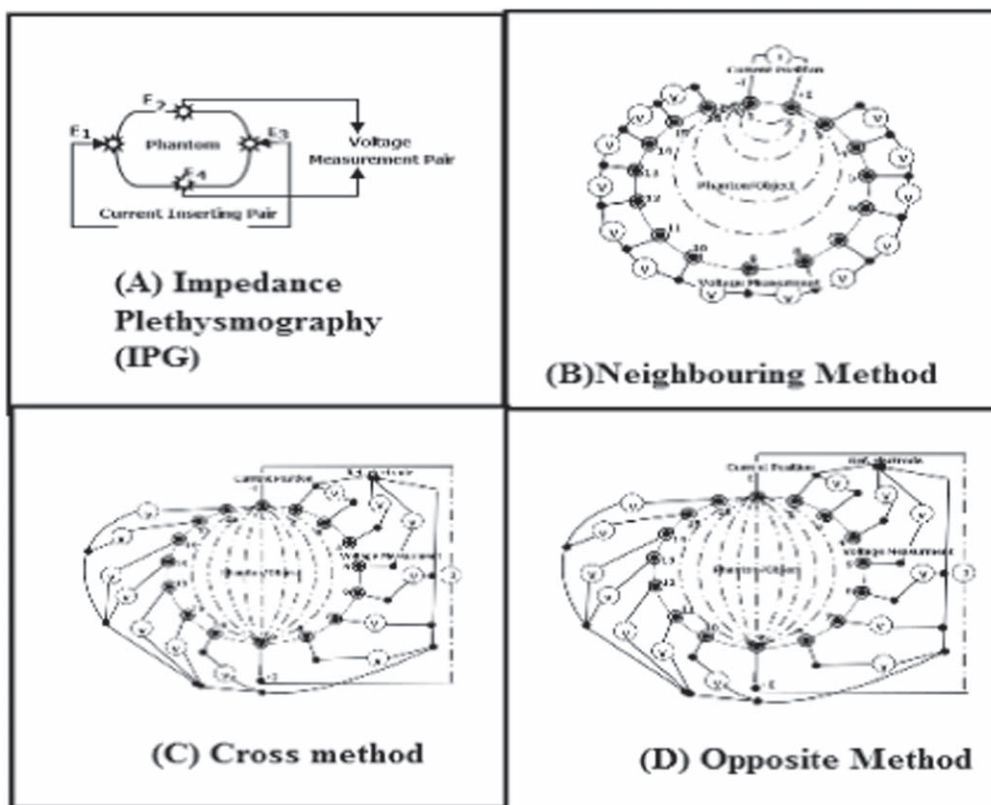


Figure 2. Methods of Bio-impedance technique for impedance-based data collection.

**Cross method.**—The cross method aims to achieve a more uniform current distribution by injecting current between electrodes further apart. In this method, adjacent electrodes are chosen as reference points for current injection and voltage measurement. For instance, in Fig. 2c, electrodes 16 and 1 are selected as the current and voltage reference electrodes, respectively. The current is first applied through electrode 2, and the voltage is measured sequentially for all other 13 electrodes with electrode 1 as the reference, as shown in Fig. 2c. This process is repeated with electrode 4 as the current electrode, followed by 6, 8, and so on, until electrode 14. This results in a total of 7 sets of 13 voltage measurements, or 91 measurements in total.

However, due to the principle of reciprocity, where swapping current and voltage electrodes yields the same results, only 104 of these measurements are truly independent. The measurement sequence is then repeated using different pairs of electrodes as reference points. For example, electrodes 3 and 2 are used as current and voltage references (Fig. 2c), followed by 5 and 2 (Fig. 2c), and finally 9, 11, and so on, until electrode 1. This step also generates 91 measurements, but again, only 104 are independent. While the cross method may not offer as high sensitivity in the peripheral regions compared to the neighbouring method, it provides better overall sensitivity across the entire area of interest.

**Opposite method.**—This method uses two diametrically opposite electrodes for current injection, such as electrodes 16 and 8 in Fig. 2d. The electrode adjacent to the current-injecting electrode acts as a voltage reference. Voltage is then measured from all remaining electrodes, excluding the current-injecting electrode itself. This process is repeated with a new pair of diametrically opposed electrodes. For example, in Fig. 2d. Electrodes 1 and 9 are used for current injection. With 16 electrodes, this approach yields a total of 8 sets of 13 voltage measurements, resulting in 104 data points. This method achieves a more uniform current distribution throughout the object, leading to good overall sensitivity for image reconstruction.

**Experimental setup.**—The experimental setup involved constructing an image of a phantom object. Electrodes were positioned around the circumference of a plastic pipe representing the phantom. A function generator was used to apply current to the electrodes, and the voltage at other electrodes was measured using a multimeter with an opposing method. For the simulation, a two or three-dimensional circular phantom with a diameter of 12.5 cm was created. A circular finite element model was employed, consisting of a specific number of nodes and elements. Sixteen equidistantly spaced nodes, marked with bold lines, served as the electrodes, such as shown in Fig. 3.

To configure the system, the following hardware components are required: a phantom, which is a closed plastic pipe, and a function generator to generate the necessary signal. A multimeter is needed to measure the value of electricity, while 16 nails will serve as electrodes. Wires, probes, and a breadboard will help connect the components. A conductivity measuring instrument will be used to determine the conductivity of the product. Furthermore, dust, salt, and water are needed as raw materials for the experiment. The setup also requires the necessary power supply, a V-I converter to convert



**Figure 3.** Experimental Setup for Industrial Type Phantom.



**Figure 4.** Industrial Monitoring Using Circular Phantom with and Without Object Detection.

voltage to current, and signal conditioning equipment to process the signals generated during the test.

**Phantom and electrode configuration.**—Constructing a suitable phantom for EIT imaging was a crucial initial step. The phantom material needed to be transparent to EIT measurements, allowing the imaging system to focus on the internal objects of interest. This phantom served as a tool for developing a reliable data processing protocol for 3D EIT object scanning. Sixteen electrodes were utilized and positioned according to a specific configuration on the phantom shown in Fig. 4. Theoretically, increasing the number of electrodes allows for more independent measurements, leading to a better constrained system, higher confidence in the results, and improved resolution of the reconstructed resistivity distribution. However, practical limitations in wiring complexity restrict the number of electrodes that can be manually attached.

The phantom used in the system has the following specifications: it has a diameter of 12.5 cm, providing a substantial internal space for the experiment. The thickness of the phantom is 0.4 cm, ensuring durability while maintaining a manageable weight. The length of the phantom is 42 cm, which allows for an extensive area for the placement of electrodes and other components needed for the conductivity measurements and other experimental procedures.

**Data acquisition and measurement.**—The EIT data acquisition system in this experiment is similar to the system used by Polyrides (2002) and Weereld et al. (2001) and the author.<sup>31</sup> It includes the use of a computer with sufficient processing power and sufficient memory for data acquisition, a continuous current source, and a matrix/multiplexer system for current exchange and voltage measurements. Voltage data were collected by measuring the potential across all electrodes when current was applied to specific opposing electrodes. The system then switched the current to another electrode and measured the voltage again. A total of 104 measurements were collected with 16 electrodes, with 16 voltage measurements for each current pair. The figure shows an example of the numbering scheme for the top electrode ring, such as shown in Fig. 5.

In this configuration, current is initially applied through electrodes 1 and 9, as shown in the figure. The voltage difference between electrodes 1 and 2 is measured and stored. In advanced systems, the current direction is reversed, and the voltage difference

**Table I. Opposite method for Plastic circular pipe.**

I/p	Outputs(mV)												
1-9	3	4	5	6	7	8	10	11	12	13	14	15	16
Ref. 2	2.34	2.40	2.45	2.47	2.50	2.52	2.41	2.61	2.65	2.60	2.60	2.5	2.54
2-10	4	5	6	7	8	9	11	12	13	14	15	16	1
Ref. 3	2.58	2.39	2.62	2.44	2.43	2.45	2.43	2.50	2.49	2.52	2.58	2.5	2.50
3-11	5	6	7	8	9	10	12	13	14	15	16	1	2
Ref. 4	2.45	2.58	2.56	2.55	2.62	2.54	2.58	2.55	2.63	2.64	2.56	2.62	2.60
4-12	6	7	8	9	10	11	13	14	15	16	1	2	3
Ref. 5	2.61	2.57	2.59	2.75	2.68	2.64	2.64	2.68	2.67	2.61	2.71	2.74	2.61
5-13	7	8	9	10	11	12	14	15	16	1	2	3	4
Ref. 6	2.48	2.55	2.69	2.68	2.65	2.63	2.64	2.67	2.68	2.81	2.87	2.88	2.65
6-14	8	9	10	11	12	13	15	16	1	2	3	4	5
Ref. 7	2.39	2.40	2.53	2.54	2.50	2.43	2.42	2.49	2.30	2.41	2.40	2.33	2.19
7-15	9	10	11	12	13	14	16	1	2	3	4	5	6
Ref. 8	2.33	2.48	2.40	2.37	2.37	2.34	2.33	2.47	2.53	2.50	2.43	2.31	2.30
8-16	10	11	12	13	14	15	1	2	3	4	5	6	7
Ref. 9	2.04	2.05	2.02	2.18	2.19	2.21	2.24	2.26	2.26	2.20	2.08	2.12	1.99

**Table II. Plastic pipe 1 Opposite method (Plastic circular pipe +Duster) 3 mA, 2 KHz.**

I/p	Outputs(mV)												
1-9	3	4	5	6	7	8	10	11	12	13	14	15	16
Ref. 2	400	440	500	490	530	430	460	520	640	710	720	680	630
2-10	4	5	6	7	8	9	11	12	13	14	15	16	1
Ref. 3	450	580	550	590	510	470	550	570	680	700	680	600	270
3-11	5	6	7	8	9	10	12	13	14	15	16	1	2
Ref. 4	450	490	550	480	420	470	450	580	590	590	540	340	279
4-12	6	7	8	9	10	11	13	14	15	16	1	2	3
Ref. 5	340	470	430	310	260	370	450	470	460	440	310	270	240
5-13	7	8	9	10	11	12	14	15	16	1	2	3	4
Ref. 6	470	540	470	450	420	490	920	530	410	430	450	430	310
6-14	8	9	10	11	12	13	15	16	1	2	3	4	5
Ref. 7	400	390	380	380	420	790	390	320	360	380	400	310	290
7-15	9	10	11	12	13	14	16	1	2	3	4	5	6
Ref. 8	550	570	550	630	580	520	500	470	480	480	410	370	320
8-16	10	11	12	13	14	15	1	2	3	4	5	6	7
Ref. 9	440	410	490	400	340	380	320	360	330	360	300	310	240

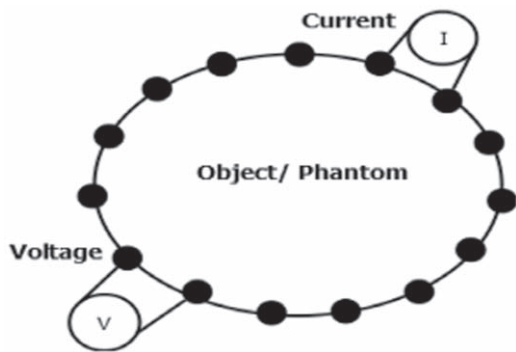


**Figure 5. Electrode Arrangements on Phantom Surface.**

between electrodes 1 and 2, and between electrodes 2 and 3, is also measured. This provides a voltage measurement for both current flow directions between two adjacent electrodes. The current injection then moves to the next pair, electrodes 2 and 10. After completing a full EIT scan, two sets of voltage data are collected: one with normal current flow and one with reversed current flow. Each set contains 104 voltage measurements, resulting in a total of

208 measurements for the entire scan of EIT, such as shown in Table I (Without object) and Table II (With object).

### Imaging Algorithm

MATLAB is a powerful and versatile language designed for industrial computing. It combines mathematics, visualization, and programming in an intuitive environment, allowing users to communicate problems and solutions using familiar mathematical notation.<sup>31</sup> This versatility makes it the preferred choice for projects such as: Mathematical and computational work: MATLAB excels in numerical calculations, making it ideal for solving complex equations and performing various mathematical operations. Next is the Algorithm development: The language facilitates the creation of algorithms for solving specific problems efficiently. Second is the data acquisition, modeling, and simulation: MATLAB provides tools for acquiring data, building models, and simulating real-world phenomena. And data analysis, exploration, and visualization: It offers comprehensive capabilities for analyzing, exploring, and visualizing data in various forms. For the scientific and engineering graphics: Creating high-quality scientific and engineering visualizations is readily achievable within MATLAB. And the application development: The platform allows for building applications, including those with graphical user interfaces.<sup>31-33</sup>

**Table III. EIT processing varies steps.**

For 1: Number of EIT scans	
Create Electrode Model	Create 16 electrode FEM Model of phantom and with homogeneous data
Solve forward problem	Solve for voltage distribution with Electrode
Load (storage normal)	Load real voltage measurements
Create inverse Electrode model	Same as electrode model expect less finite elements
Solve inverse problem	Solve for voltage distribution using the inverse electrode model, forward voltage measurements, and the real voltage measurements.
End	

One of MATLAB's key strengths is its interactive nature and the use of arrays as its fundamental data element. This eliminates the need for explicit dimensioning, significantly reducing the time required to solve technical computing problems compared to traditional scalar languages like C or Fortran. Over the years, MATLAB has evolved significantly, incorporating feedback from a vast user base. Furthermore, MATLAB boasts a rich ecosystem of add-on toolboxes catering to specific application areas. These toolboxes, essentially collections of specialized MATLAB functions, empower users to learn and apply advanced technologies in various fields like signal processing, control systems, neural networks, and many more.

Evaluating MATLAB-based algorithms under diverse conditions reveals their strengths and potential limitations. MATLAB excels in rapid prototyping due to its user-friendly interface and extensive library of built-in functions, which facilitate quick development and testing of algorithms.<sup>31</sup> This flexibility allows researchers to efficiently iterate on design and implement complex models with relatively minimal coding effort. However, while MATLAB is powerful for prototyping and small to medium-scale applications, its performance can be limited in large-scale applications due to computational inefficiencies and higher memory usage. In such cases, MATLAB's execution speed and scalability may fall short compared to more specialized or lower-level programming environments optimized for high-performance computing. Addressing these limitations often requires integrating MATLAB with more robust computational tools or optimizing the algorithm's implementation to handle larger datasets and more intensive processing demands effectively.<sup>32,33</sup>

**Eidors toolkit.**—EIDORS aims to foster collaboration among researchers working on Electrical Impedance Tomography (EIT) and Diffusion-based Optical Tomography (DOT), both in medical and industrial applications. EIDORS3D is a software suite specifically designed for image reconstruction in these fields. Its core objective is to provide freely accessible and modifiable software for reconstructing images from electrical or diffuse optical data. This software plays a crucial role in advancing research by offering: A reference implementation for comparison and evaluation of new developments in image reconstruction algorithms. With the functional software base for building upon and testing new ideas.<sup>31</sup>

The original EIDORS software (Vauhkonen et al., 2000) stemmed from Vauhkonen's thesis work (1997).<sup>7</sup> It included a MATLAB package for 2D mesh generation, solving the forward problem, and reconstructing and displaying images. To address the need for 3D reconstruction capabilities, a new project, EIDORS3D, was initiated (Polydorides and Lionheart, 2002), based on the software developed for Polydorides' thesis (2002). Both EIDORS software packages share the same numerical foundation, utilizing finite element representation for media and employing regularized inverse techniques for image reconstruction.<sup>31–33</sup>

Observations from three years of EIDORS3D usage revealed common patterns: researchers typically downloaded the software, ran provided examples, and made modifications to suit their specific needs. However, the lack of a modular structure in EIDORS3D led to changes being directly integrated into the code, often resulting in

duplicated and difficult-to-contribute code.<sup>34–37</sup> Additionally, research focus has shifted beyond basic reconstruction algorithms, towards areas like mesh generation, electrode modeling, visualization, and error detection. Modular components readily integrated with various reconstruction algorithms would significantly facilitate these advancements.<sup>37–40</sup>

**EIT algorithm processing.**—The data processing component of EIT has made substantial progress in both medical and non-medical areas, which was critical for this trial. The work of Polidorides (2002) is particularly important because it successfully addressed the data processing challenges inherent in soft-field tomography.<sup>24</sup> His contributions led to the development of the MATLAB toolkit EIDORS (Electrical Impedance Tomography and Diffuse Optical Tomography Reconstruction Software). EIDORS is a MATLAB framework developed in collaboration with EIT research groups to enhance the overall EIT research community.<sup>34,35</sup>

In EIT solving the inverse problem is crucial for reconstructing the intrnal conductivity distribution of a body from surface electrical measurements. The mathematical framework and system for dealing with this evolving problem is fundamental to the EIT approach. The forward problem involves calculating theinteal potential measurements given a known conductivity distribution.<sup>31–33</sup> The governing equations for the forward problem are derived from Maxwell's equations, specifically focusing on the Laplace equation for DC measurements:

$$\nabla \cdot (\sigma \nabla V) = 0 \quad [1]$$

Where  $\sigma$  the conductivity distribution and  $V$  is the electrical potential. For a given conductivity distribution  $\sigma$ , this equation can be solved using FEM or other numerical techniques to compute the voltage measurements on the boundary.

The inverse problem aims to reconstruct the conductivity distribution  $\sigma$  from the measured voltage data  $V_m$  on the boundary.<sup>31</sup> This is typically framed as an optimization problem:

$$\sigma \text{ Minimizes } \|V_m - V_{calc}(\sigma)\|^2 \quad [2]$$

Where  $V_{calc}(\sigma)$  represents the calculated voltage measurements from the forward problem for a given conductivity  $\sigma$ , and  $\|\cdot\|^2$  denotes the squared norm, measuring the discrepancy between measured and calculated voltages.

The solution of the inverse problem in EIT addresses the nonlinear optimization challenge aimed at estimating the intrnal conductance distribution from boundary measurements. Iterative linearization methods such as the Gauss-Newton or Levenberg-Marquart methods are used to solve conductance estimates through a series of approximations and regularization methods are used to deal and stabilize the solution. Different optimization algorithms are used to further solve these estimates. Together, these mathematical concepts and algorithms underlie the reconstruction of intrinsic conductance images in EITs.

The Table III describes the steps for processing information from an Electrical Impedance Tomography (EIT) scan. It begins with a basic computer model for the electrodes used during scanning, and the neurons that are assumed to be identical throughout. Next, it

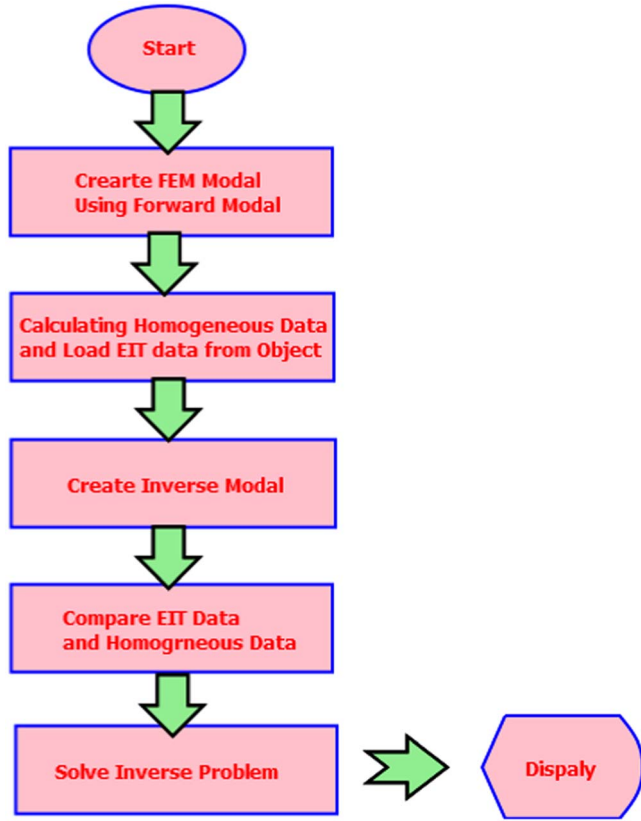


Figure 6. Imaging Algorithm Flow chart.

plots the expected voltage distribution based on this model. Then, the actual voltage measurements made during the scan are loaded. Finally, an optimized model with fewer components is constructed, and the actual force measurements are added to the simulated results to correct for the force distribution in the body which is perfect. This process likely contributes to meaningful conclusions from the raw EIT scan data. And also shown the flow chat of the deigned reconstruction for the EIT obtained data, such as shown in Fig. 6.

**Results and Analysis**

The experiment utilized a method of driving and measuring voltages to obtain EIT images. A proximity driving and measuring system was used, where a current was applied between each of two adjacent electrodes and the difference in output voltage was measured at the other electrodes. Complete measurements were performed with a total of 16 electrodes in one plane as stimulating electrodes. Figures 7 and 8 shows the impedance distribution curves measured for all 16 electrodes. These measurements were collected with an applied signal frequency of 50 kHz.

According to the analytical view of obtained data (Table I), shown in the Table IV of all parametrical analyses for EIT obtained such s like maximum, minimum, variance, average, standard deviation, etc these parametric analyses are shown in Figs. 9 and 10. And data table of this parametric value is shown in Table IV of the Analytical analysis of the experimental work of Plastic circular pipe.

In other case second for experimental work of Plastic circular pipe with object, complete measurements were performed with a total of 16 electrodes in one plane as stimulating electrodes. Figures 11 and 12 shows the impedance distribution curves

**Impedance Distribution Graph**

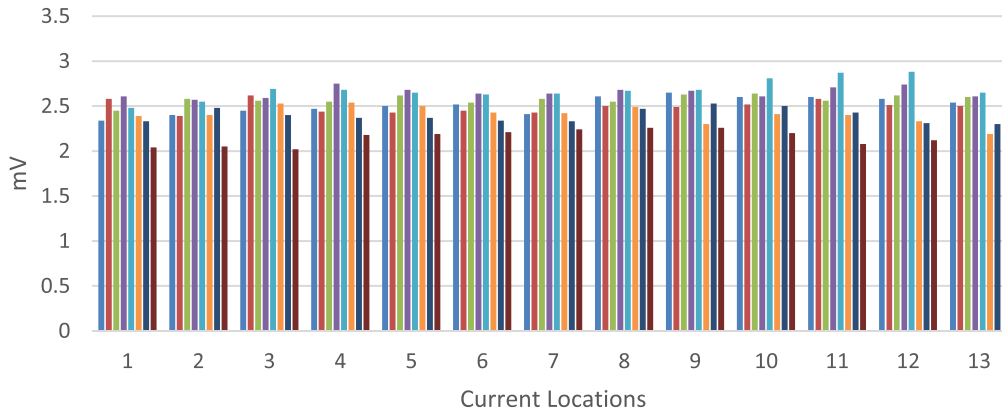


Figure 7. Impedance distribution Graph for all current locations for phantom.

**Table IV. Analytical analysis of the experimental work of Plastic circular pipe.**

	V1	V2	V3	V4	V5	V6	V7	V8	V9	V10	V11	V12	V13
Min	2.0400	2.0500	2.0200	2.1800	2.1900	2.2100	2.2400	2.2600	2.2600	2.2000	2.0800	2.1200	1.9900
Q1	2.3375	2.3975	2.4375	2.4225	2.4150	2.4075	2.3900	2.4850	2.4425	2.4775	2.4225	2.3250	2.2725
Median	2.4200	2.4400	2.5450	2.5050	2.5000	2.4850	2.4250	2.5250	2.5800	2.5600	2.5700	2.5450	2.5200
Q3	2.5050	2.5550	2.5975	2.5825	2.6275	2.5625	2.5950	2.6250	2.6550	2.6175	2.6275	2.6500	2.6025
Max	2.6100	2.5800	2.6900	2.7500	2.6800	2.6400	2.6400	2.6800	2.6800	2.8100	2.8700	2.8800	2.6500
var.	0.0319	0.0295	0.0434	0.0318	0.0267	0.0212	0.0214	0.0183	0.0277	0.0323	0.0551	0.0616	0.0563
Avg	2.4025	2.4275	2.4825	2.4975	2.4925	2.4700	2.4613	2.5288	2.5263	2.5363	2.5288	2.5113	2.4225
Range	0.5700	0.5300	0.6700	0.5700	0.4900	0.4300	0.4000	0.4200	0.4200	0.6100	0.7900	0.7600	0.6600
Dav.	0.1787	0.1719	0.2082	0.1784	0.1633	0.1456	0.1461	0.1352	0.1664	0.1796	0.2347	0.2482	0.2374
St. Dv.	0.1672	0.1608	0.1948	0.1669	0.1528	0.1362	0.1367	0.1264	0.1556	0.1680	0.2196	0.2322	0.2220



Figure 8. Impedance distribution Graph for one current location for phantom.

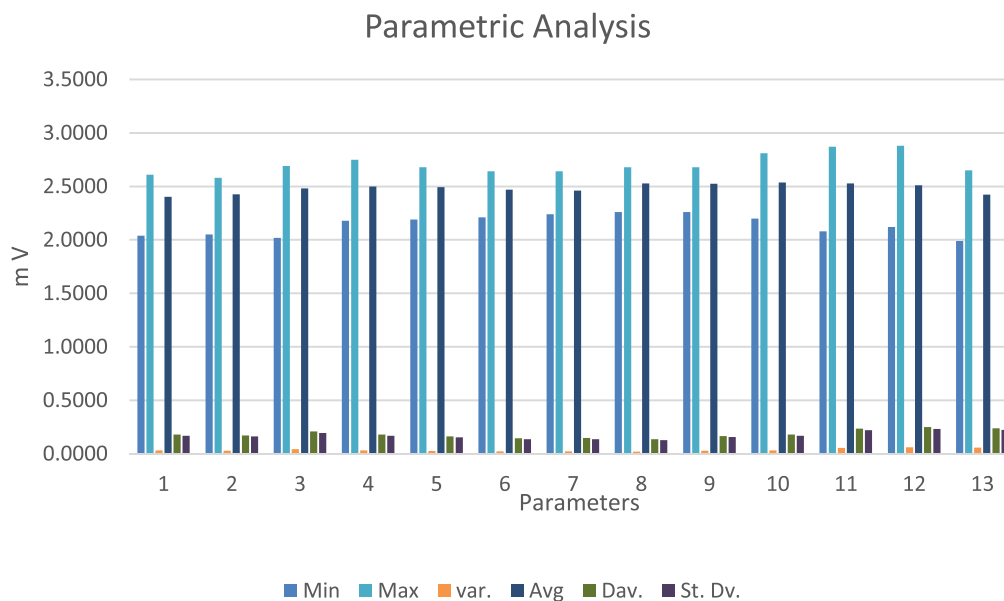


Figure 9. Parametric Analysis (Max, Min, Average, Deviation, Variance, St. Deviation) for opposite method according to 16 Electron configuration of the phantom.

Table V. Analytical analysis of the experimental work of Plastic circular pipe with object.

	V1	V2	V3	V4	V5	V6	V7	V8	V9	V10	V11	V12	V13
Min	3.4000	3.9000	3.8000	3.1000	2.6000	3.7000	3.2000	3.2000	3.3000	3.6000	3.0000	2.7000	2.4000
Q1	4.0000	4.3250	4.6000	3.9500	4.0000	4.1750	4.3500	4.4250	3.9750	4.1750	3.7750	3.1000	2.6250
Median	4.4500	4.8000	4.9500	4.6500	4.2000	4.7000	4.5500	4.9500	4.7000	4.6000	4.3000	3.5500	2.8450
Q3	4.5500	5.4750	5.5000	5.1500	5.1500	4.9750	5.1250	5.4000	6.0250	6.1750	5.7500	4.7250	3.1250
Max	5.5000	5.8000	5.5000	6.3000	5.8000	7.9000	9.2000	5.8000	6.8000	7.1000	7.2000	6.8000	6.3000
var.	0.3764	0.5170	0.3857	1.1341	1.0857	1.7400	3.2829	0.8907	1.6913	1.9155	2.4941	2.2198	1.6291
Avg	4.3750	4.8625	4.9000	4.6625	4.3500	4.9000	5.0500	4.7750	4.9375	5.1125	4.7625	4.1375	3.2238
Range	2.1000	1.9000	1.7000	3.2000	3.2000	4.2000	6.0000	2.6000	3.5000	3.5000	4.2000	4.1000	3.9000
Dav.	0.6135	0.7190	0.6211	1.0649	1.0420	1.3191	1.8119	0.9438	1.3005	1.3840	1.5793	1.4899	1.2764
St. Dv.	0.5739	0.6726	0.5809	0.9962	0.9747	1.2339	1.6948	0.8828	1.2165	1.2946	1.4773	1.3937	1.1939

measured for all 16 electrodes. These measurements were collected with an applied signal frequency of 50 kHz.

According to the analytical view of obtained data (Table II), shown in the Table V of all parametrical analyses for EIT obtained

such s like maximum, minimum, variance, average, standard deviation, etc these parametric analyses are shown in Figs. 13 and 14. And data table of this parametric value is shown in Table V of the Analytical analysis of the experimental work of Plastic circular pipe.

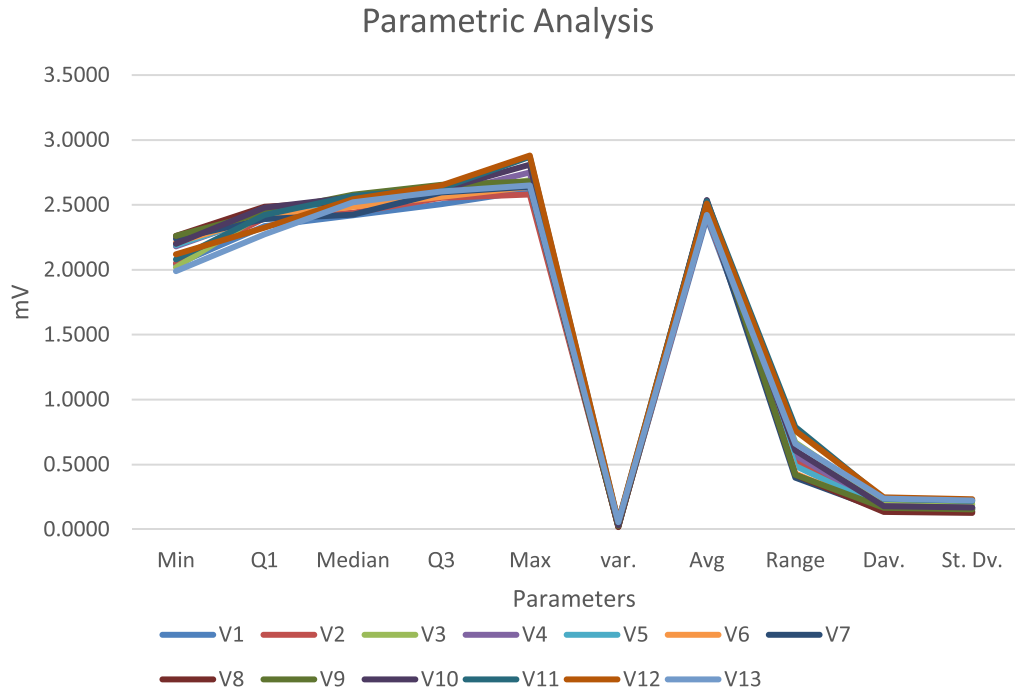


Figure 10. Parametric Analysis (All Parameters) for opposite method according to 16 Electron configuration of the phantom.

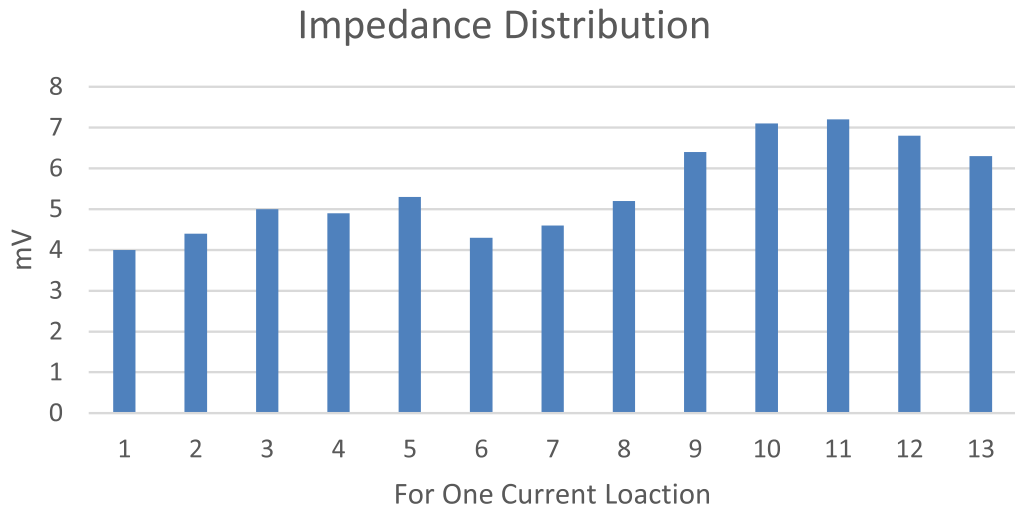


Figure 11. Impedance distribution Graph for one current location of the phantom.

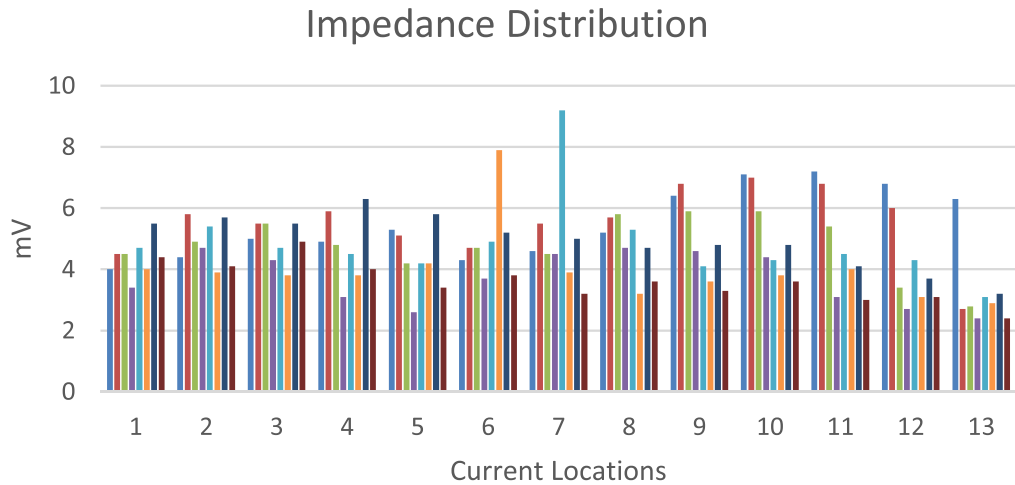
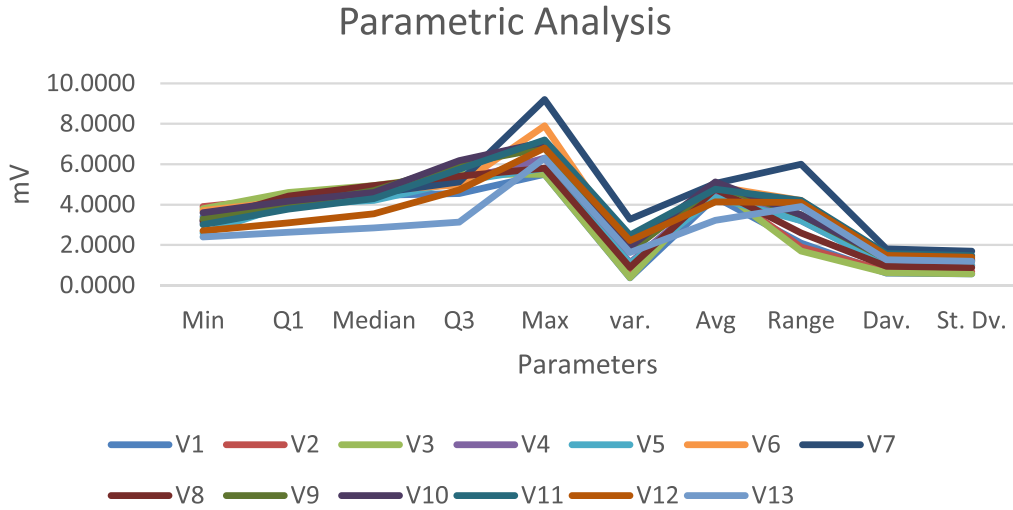
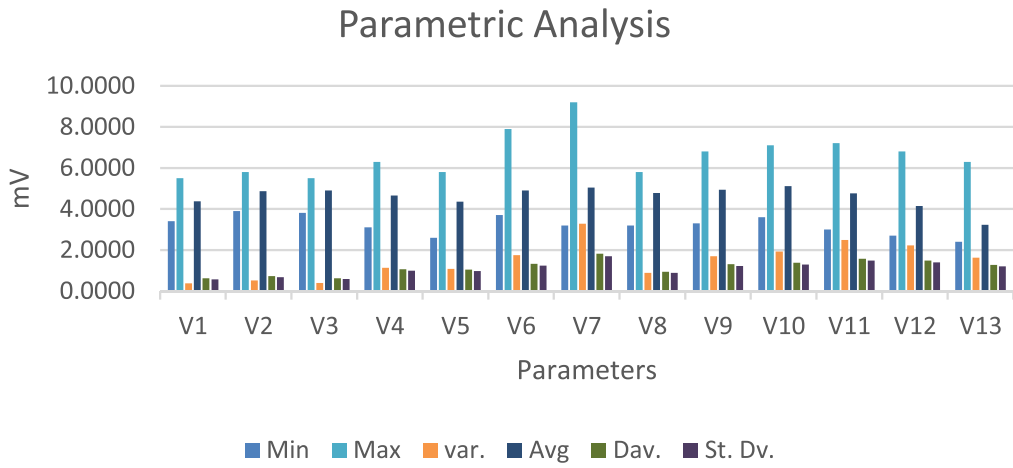


Figure 12. Impedance distribution Graph for all current locations for the phantom.



**Figure 13.** Parametric Analysis (All Parameters) for opposite method according to 16 Electron configuration of the phantom.



**Figure 14.** Parametric Analysis (Max, Min, Average, Deviation, Variance, St. Deviation) for opposite method according to 16 Electron configuration of the phantom.

**Simulation results.**—The simulation utilized a simplified two-dimensional, isotropic cross-section of a phantom tank containing a cylindrical object with a diameter of 12.5 cm. This served as the model for reconstructing the impedance image of the object using different data collection methods. The conventional adjacent method, which only acquires 104 data points, was shown to suffer significantly from the ill-posed problem inherent in EIT image reconstruction. This limitation is likely due to the insufficient amount of data collected.

**Meshes and forward computations.**—The forward solution includes the potential inside the domain and voltages on the electrodes. The potential distributions were computed using the mesh as shown in Fig. 15. The placements of the electrodes are clearly visible.

Meshing is a crucial component in EIT because it significantly impacts both the accuracy and computational efficiency of the imaging process. By dividing the domain into smaller, discrete elements, meshing allows for a detailed representation of the physical geometry of the object being imaged, which is essential for accurately solving the forward problem and computing electrical potentials based on conductivity distribution. The resolution of the mesh directly affects solution precision, with finer meshes capturing

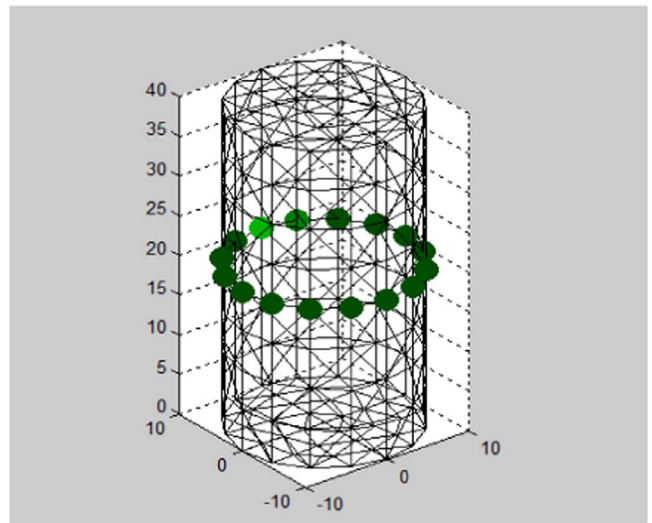


**Figure 15.** Meshes and forward computations of the Circular Phantom.

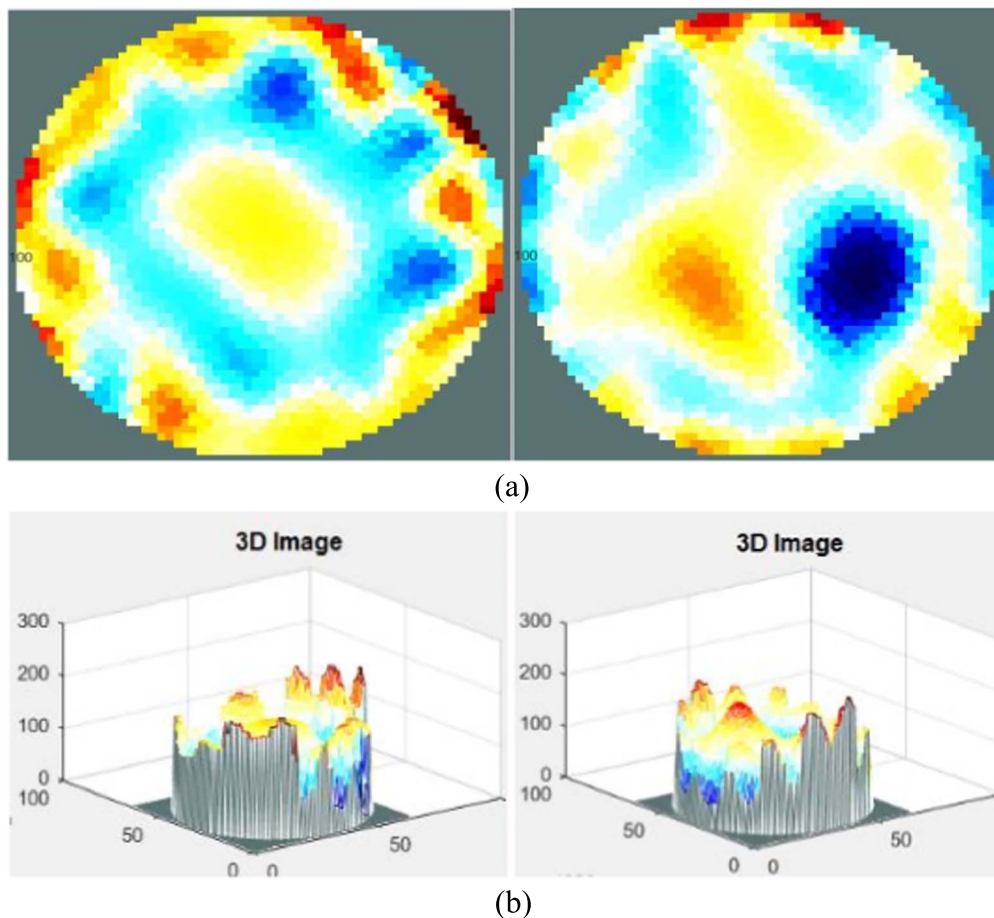


**Figure 16.** (a) Internal Structure in 2D Image for the Circular Phantom. Figure 16b Internal Structure in 3D Image for the Circular Phantom.

more detail and leading to more accurate internal reconstructions, while coarser meshes may miss subtle variations. Proper meshing also enhances numerical stability, reducing errors and artifacts in computational algorithms, and influences computational efficiency, balancing detail with resource demands to ensure timely analysis. Furthermore, the quality of the mesh is vital for effectively solving the inverse problem, where accurate reconstruction of the conductivity distribution relies on a well-structured mesh. Overall, meshing is fundamental to achieving precise, stable, and efficient EIT imaging, making its careful optimization essential for advancing EIT technology and its diverse applications.

*Final image.*—The final stage for simulation results in the 2D/3D image. The Figs. 16a 16b is based on the number of finite elements. As the number of finite elements are increases, the image becomes clearer.

While the existing MATLAB functions offer a convenient platform for rapid prototyping and testing of various EIT reconstruction schemes due to their ease of use and visualization capabilities, they often suffer from performance limitations when dealing with large-scale problems. This is because MATLAB is an interpreted language, and its execution speed can be significantly slower compared to compiled languages. Therefore, for final applications involving large dimensional datasets, rewriting the computationally intensive reconstruction algorithms is often necessary to achieve optimal performance.

### Discussion

EIT offers a versatile imaging technique for a variety of industrial and medical applications. Its main function is to reconstruct internal impedance distributions, usually focusing on resistivity, by solving

the inverse problem. This capability enables real-time monitoring, making EIT suitable for continuous data acquisition in dynamic applications. Increasing the number of electrodes improves image quality, which benefits both engineering and medicine. As researchers better understand the limitations of EIT, it holds promise for a variety of scales and applications: examining geothermal effects in laboratory studies, monitoring lake conditions for insights into geothermal processes, and optimization methods e.g its recharge in ponds. Combining EIT data with tools such as LabVIEW facilitates image reconstruction, aided by system manipulation using techniques such as the Finite Difference Method (FDM) and programming languages. EIT is widely used in industrial design modeling, especially in the visualization of conducting fluids, a technique known as Electrical Resistance Tomography (ERT). In ERT, metal electrodes directly contact the fluid, while the principles of data acquisition and reproduction are similar to those in medicine. This versatile approach supports various industrial applications such as on-line monitoring of equipment such as hydraulic conveyors, separators, and mixers, enhancing process control and design, and validating computational fluid dynamics simulations for accuracy. EIT also plays an important role in laboratory research and education, facilitating both research efforts and teaching activities. EIT made great strides in medical imaging, focusing on specific areas such as the central nervous system to study the brain and measure scalp resistance, look at the lungs of air into the respiratory system, and regulates gastric emptying of food. In addition to medical applications, geophysics uses a related technique called electrical impedance tomography, using electrodes in surfaces or cavities to detect resistivity anomalies and, in engineering system monitoring, electronic arrays for monitoring permeable mixtures in pipes. EIT are composed to significantly transform both theoretical

and practical aspects of this imaging technique. By improving resolution and accuracy through advanced algorithms and mathematical formulations, EIT can offer more detailed and precise insights into internal structures, which is critical for applications in medical diagnostics and industrial process monitoring. The broader industrial applications of these findings have the potential to revolutionize process monitoring, tank inspections, and pipeline analysis, leading to enhanced safety, efficiency, and reliability in various sectors. The successful translation of these advancements into real-world solutions will depend on collaborative efforts to integrate EIT technology into existing systems, conduct rigorous field testing, and develop cost-effective solutions. As these challenges are addressed, the full potential of EIT to drive innovation and improve operational outcomes across diverse industries will be realized.

### Conclusions

Bio-impedance technique (or EIT) is a versatile imaging technique with applications in both medical and non-medical fields. Its core function lies in reconstructing the internal impedance distribution (often focusing on resistivity) by solving the inverse problem. This experimental study demonstrated the forward problem of calculating potential distribution using the Finite Element Method through the Industrial Phantom. A phantom model was utilized, and reconstruction algorithms were designed using MATLAB based Algorithm. Data acquisition for these algorithms was achieved through dedicated software and hardware. While Algorithm offers a convenient platform for rapid prototyping of various EIT reconstruction schemes due to its ease of use and visualization capabilities, its performance can be hindered in large-scale problems. EIT remains an attractive option due to its non-ionizing nature and affordability, making it a valuable addition to the medical and non-medical imaging landscape.

### Future Direction

To address current limitations and expand the applications of Electrical Impedance Tomography (EIT), future research must focus on several key areas. Enhancing imaging resolution and accuracy through advanced meshing techniques, adaptive mesh refinement, and innovative computational algorithms will improve the detection of fine details and anomalies. Integrating EIT with other imaging modalities, such as MRI or CT, could offer more comprehensive views of internal structures, particularly benefiting medical diagnostics and industrial applications. Additionally, developing real-time processing capabilities and miniaturized, wearable EIT systems will enable more immediate feedback and personal health monitoring.

Exploring novel applications in emerging fields like bioengineering, material science, and environmental monitoring holds the potential to uncover new uses for EIT technology. Addressing computational challenges by creating efficient algorithms and leveraging machine learning will enhance image reconstruction and interpretation. Long-term experimental research and the establishment of standardized protocols are crucial for validating and refining new EIT technologies, ensuring their effectiveness and reliability in various applications. By pursuing these research directions, EIT technology can be significantly advanced, offering greater precision and broader utility across different fields.

### Acknowledgments

The Authors would like to thank the department DICE, CUIET, Chitkara University, Punjab for providing useful infrastructure and support to carry out various experiments related to this paper. Author Ramesh Kumar, expresses gratitude to the Science and Engineering Research Board and acknowledge the Science and Engineering Research Board (SERB) (EEQ/2023/000899) Department of Science and Technology (DST), Government of India for their financial

assistance. Author Ratneshwar Kumar Ratnesh also expresses gratitude to the Science and Engineering Research Board (SERB) (TAR/2022/000618), Department of Science and Technology (DST), Government of India for their financial assistance.

### Author Contribution

Ramesh Kumar: Main author, developed most of the theory presented in the paper, conduct experiment, and wrote the paper. Ratneshwar Kumar Ratnesh: has also consider as main author, developed most of the theory presented in the paper, conducted experiments, analysed the data, and wrote the paper. Rajeew Kumar Chauhan: has third author and he contributed formulating and correcting the paper. Ashok Kumar: has fourth author and he contributed formulating and correcting the paper. Manish Kumar Singla: has fifth author and he contributed formulating and correcting the paper. Ramji Gupta: has sixth author and he contributed as, formulating, and correcting the paper.

### Funding

Not applicable.

### Compliance with Ethical Standards Conflict of Interest

The authors declare that they have no conflict of interest.

### Code Availability

Not applicable.

### Ethics Approval

Not applicable.

### Consent to Participate

Not applicable.

### Consent for Publication

Not applicable.

### Replication of Results

Not Presented.

### ORCID

Ratneshwar Kumar Ratnesh  <https://orcid.org/0000-0002-3438-6541>

### References

1. R. W. Stacey, K. Li, and R. N. Horne, "Investigating electrical-impedance tomography as a technique for real-time saturation monitoring." *SPE J.*, **14**, 135 (2009).
2. K. G. Boone and D. S. Holder, "Current approaches to analogue instrumentation design in electrical impedance tomography." *Physiol. Meas.*, **17**, 229 (1996).
3. D. S. Holder, "Electrical impedance tomography (EIT) of brain function." *Brain Topogr.*, **5**, 87 (1992).
4. R. K. Meena, S. K. Pahuja, A. B. Queyam, and A. Sengupta, "Electrical impedance tomography: a real-time medical imaging technique." *Handbook of Research on Advanced Concepts in Real-Time Image and Video Processing*, IGI Global 130 (2018).
5. A. J. Peyton, "3 - Electromagnetic induction tomography." *Industrial tomography Systems and Applications*, **0**, 61 (2015).
6. A. B. Queyam, R. Kumar, R. K. Ratnesh, and R. K. Chauhan, "LabVIEW-enabled synthetic signal for empowering fetal-maternal healthcare." *ECS J. Solid State Sci. Technol.*, **13**, 057005 (2024).
7. M. Vauhkonen, W. R.-B. Lionheart, L. M. Heikkinen, P. J. Vauhkonen, and J. P. Kaipio, "A MATLAB package for the EIDORS project to reconstruct two-dimensional EIT images." *Physiol. Meas.*, **22**, 107 (2000).
8. A. Garg, R. K. Ratnesh, R. K. Chauhan, N. Mittal, and H. Shankar, "Current advancement and progress in BioFET: a review." *International Conference on Signal and Information Processing (ICONSIP)* (IEEE, Pune, India) 1 (2022).
9. S. R. Kothiyal, R. K. Ratnesh, and A. Kumar, "Field effect transistor (FET)-sensor for biological applications." *International Conference on Device Intelligence, Computing and Communication Technologies (DICCT)*, **2023**, 433 (2023), IEEE.

10. R. K. A. Garg, "Ratnesh, solar cell trends, and the future: a review." *Journal of Pharmaceutical Negative Results*, **13**, 2051 (2022).
11. R. Kumar, S. Kumar, and A. Sengupta, "Optimization of bio-impedance techniques-based monitoring system for medical & industrial applications." *IETE J. Res.*, **68**, 3843 (2020).
12. G. Xu, R. Wang, S. Zhang, S. Yang, G. A. Justin, M. Sun, and W. Yan, "A 128-electrode three dimensional electrical impedance tomography system." *Proc. 29th Annu. Int. Conf. IEEE EMBS* 4386 (2007), PMID: 18002976.
13. F.-M. Yu, C.-N. Huang, F.-M. Hsu, and H.-Y. Chung, "Pseudo electrodes driven patterns for electrical impedance tomography." *SICE Annu. Conf.*, Takamatsu, Japan 2890 (2007).
14. A. D. Liston, "Models and image reconstruction in electrical impedance tomography of human brain function." *Health and Social Sciences*, Middlesex University (2003), (Doctoral dissertation, Middlesex University) <https://repository.mdx.ac.uk/item/830qv>.
15. A. Adler and R. Guardo, "Electrical impedance tomography: regularised imaging and contrast detection." *IEEE Trans. Med. Imaging*, **15**, 170 (1996).
16. R. K. Ratnesh, M. K. Singh, and J. Singh, "Enhancing ZnO/Si Heterojunction photodetector performance for ultra high responsivity across wide spectral range." *Journal of Material Science: Materials in Electronics*, **35**, 756 (2024).
17. R. K. Ratnesh, M. K. Singha, V. Kumar, S. Singh, R. Chandra, M. Singh, and J. Singh, "Mango leaves (*Mangifera Indica*) derived highly fluorescent green graphene quantum dot nanopores for enhanced on-off dual detection of cholesterol and Fe<sup>2+</sup> Ions based on molecular logic operation." *Biomaterials Science & Engineering, American Chemical Society*, **7**, 4417 (2024).
18. I. V. Denisov, Y. N. Kulchin, A. V. Panov, and N. A. Rybalchenko, "Neural network methods of reconstruction tomography problem solutions." *Journal of Optical Memory & Neural Networks*, **14**, 45 (2005), [http://canopus.iacp.dvo.ru/~panov/rev\\_nn\\_tomography.pdf](http://canopus.iacp.dvo.ru/~panov/rev_nn_tomography.pdf).
19. H. G. Han, W. Lu, Y. Hou, and J. F. Qiao, "An adaptive-PSO-based self-organizing RBF neural network." *IEEE Trans Neural Netw. Learn. Syst.*, **29**, 104 (2016).
20. M. Argyrou, D. Maintas, C. Tsoumpas, and E. Stiliaris, "Tomographic image reconstruction based on Artificial Neural Network (ANN) techniques." *IEEE Nuclear Science Symposium and Medical Imaging Conference Record (NSS/MIC)*, Anaheim, CA, USA3324 **2012** (2012).
21. M. K. Yadav, R. Kumar, R. K. Ratnesh, J. Singh, R. Chandra, A. Kumar, V. Vishnoi, G. Singh, and A. K. Singh, "Revolutionizing technology with spintronics: devices and their transformative applications." *Materials Science & Engineering B*, **303**, 117293 (2024).
22. H. A. Bruck et al., "Digital image correlation using Newton-Raphson method of partial differential correction." *Experimental Mechanics*, **29**, 261 (1989).
23. J. L. Mueller and S. Siltanen, "The D-bar method for electrical impedance tomography—demystified." *Inverse Probl.*, **36**, 093001 (2020).
24. H. Xia, Q. Shan, J. Wang, and D. Liu, "NAS powered deep image prior for electrical impedance tomography." *IEEE Trans. Comput. Imaging*, **10**, 1165 (2024).
25. I. Nur Rifai, P. A. Sejati, S. Akita, and M. Takei, "FPGA-based planar sensor electrical impedance tomography (FPGA-psEIT) system characterized by double feedback howland constant-current pump and programmable front-end measurement." *IEEE Trans. Instrum. Meas.*, **73**, 2005310 (2024).
26. R. Pietrzyk, M. Mazurek, and J. Chwałdaś-Majdańska, "Image reconstruction and bladder stimulation using electrical impedance tomography." *J. Modern Sci.*, **57**, 668 (2024).
27. R. Kumar and R. Mahadeva, "An experimental measurement and control of human body stomach using electrical impedance tomography." *J. Circuits Syst. Comput.*, **30**, 2375 (2021).
28. S. R. Kothiyal, R. K. Ratnesh, and A. K. Shukla, "Enhancing sensing with surface plasmons resonance: theoretical insights and design strategies in photonic crystal fiber." *International Conference Artificial Intelligence and Information Technologies, (ICAIT)-2023, Taylor & Francis* 279 (2024).
29. R. Kumar, S. Kumar, A. B. Queyam, and A. Sengupta, "An experimental validation of bio-impedance technique for medical & non-medical application." *8th Int. Conf. Cloud Comput. Data Sci. Eng. (Confluence)*, **2018**, 14 (2018).
30. R. Kumar, R. K. Ratnesh, J. Singh, R. Chandra, G. Singh, and V. Vishnoi, "Recent prospects of medical imaging and sensing technologies based on electrical impedance data acquisition system." *Journal of Electrochemical Society*, **170**, 117507 (2023).
31. N. Polydorides and W. R.-B. Lionheart, "A Matlab toolkit for three-dimensional electrical impedance tomography: a contribution to the electrical impedance and diffuse optical reconstruction software project." *Meas. Sci. Technol.*, **13**, 1871 (2002).
32. R. Kumar, R. Kumar Ratnesh, J. Singh, A. Kumar, and R. Chandra, "IoT-driven experimental framework for advancing electrical impedance tomography." *ECS J. Solid State Sci. Technol.*, **13**, 027002 (2024).
33. R. Kumar and S. Tripathi, "A novel GUI-based image reconstruction algorithm of EIT imaging technique." *Int. J. Cogn. Inform. Nat. Intell. (IJCINI)*, **15**, 31 (2021).
34. B. Kilic and M. Korurek, "A finite element method based neural network technique for image reconstruction in electrical impedance imaging." *Proceedings of the 1998 2nd International Conference Biomedical Engineering Days, Istanbul, Turkey* 100 (1998).
35. L. Zhang, H. Wang, Y. Xu, and D. Wang, "Image reconstruction algorithm based on 1-norm for electrical resistance tomography." *2nd International Conference on Intelligent Control and Information Processing, Harbin, China* **2011**, 277 (2011).
36. V. D. Ashwlayan, R. K. Ratnesh, D. Sharma, A. Sharma, A. Sangal, A. Saifi, and J. Singh, "A comprehensive review on plant-based medications and chemical approaches for autism spectrum disorders (ASDs) psychopharmacotherapy." *Indian Journal of Microbiology*, **0**, 1 (2024).
37. L.-F. Tanguay, H. Gagnon, and R. Guardo, "Comparison of applied and induced current electrical impedance tomography." *in IEEE Transactions on Biomedical Engineering*, **54**, 1643 (2007).
38. R. Kumar, S. Kumar, and A. Sengupta, "An experimental analysis and validation of electrical impedance tomography technique for medical or industrial application." *Biomedical Engineering: Applications, Basis and Communications*, **31**, 1950010 (2019).
39. J. L. Mueller, S. Siltanen, and D. Isaacson, "A direct reconstruction algorithm for electrical impedance tomography." *IEEE Transactions on Medical Imaging*, **21**, 555 (2002).
40. R. Kumar, S. Kumar, and A. Sengupta, "A review: electrical impedance tomography system and its application." *J. Control Instrum.*, **7**, 14 (2016).